Progress In Electromagnetics Research, Vol. 132, 71–90, 2012

EXPERIMENTAL VALIDATION OF A TDR-BASED SYSTEM FOR MEASURING LEAK DISTANCES IN BURIED METAL PIPES

A. Cataldo[1, *], G. Cannazza[1], E. De Benedetto[1], and N. Giaquinto[2]

[1]Department of Engineering for Innovation, University of Salento, via Monteroni, Lecce 73100, Italy

[2]Department of Electrical and Electronic Engineering, Politecnico di Bari, Bari 70125, Italy

Abstract—In this paper, the experimental validation of a time domain reflectometry (TDR)-based method for pinpointing water leaks in underground metal pipes is presented. The method relies on sensing the local change in the dielectric characteristics of the medium surrounding the leak point. The experimental validation of the method was carried out through measurements performed on a pilot plant (experimental case P1) and through on-the-field measurements performed on two 'already-installed pipes', i.e., already operating and connected to the water distribution system (experimental cases P2 and P3). For the pilot plant, different leak conditions were imposed and the corresponding TDR responses were acquired and analyzed. For the on-the-field measurements, TDR measurements were performed on pipes for which a leak-detection crew had preliminarily individuated the possible presence of leaks (through traditional leak-detection methods). Finally, in view of the practical implementation of the proposed TDR-based leak-detection system, a data-processing procedure (which gives an automatic evaluation of the position of the leak) is also presented.

1. INTRODUCTION

The individuation of leaks is extremely important for the optimization and rationalization of water resources. Nevertheless, the techniques that are currently used for the detection of leaks in buried pipes (which are mainly based on electro-acoustic methods), are extremely

Received 14 August 2012, Accepted 11 September 2012, Scheduled 21 September 2012

* Corresponding author: Andrea Cataldo (andrea.cataldo@unisalento.it).

time-consuming and require highly-experienced personnel [1, 2]. Additionally, traditional methods can be affected by errors in the leak localization when the measurements cannot be performed in optimal operating conditions (e.g., high hydraulic pressure in the pipeline, absence of environmental noise or interference and suitability of the pipe material to the sound propagation). As a consequence, the development of new leak detection methods is considered as the key for favoring the control and monitoring possibilities. In this regard, much research effort is constantly dedicated to the development of innovative methodologies for leak detection, also resorting to methods based on autoregressive models [3], continuous wave sensors [4], and so on.

In [5–7], the authors have described a time domain reflectometry (TDR)-based method for leak detection. TDR is a well-established monitoring technique that has been used for many different applications, such as dielectric and spectroscopic characterizations of materials [8–11]; quantitative and qualitative control of liquids [12, 13]; investigation of vegetable oils [14–16]; impedance measurements [17]; dynamic structure analysis [18, 19]; fault diagnosis on wires [20, 21]; distributed pressure profile [22]; soil moisture measurements [23–26]; characterization of electronic devices devices and components [27–30]; etc. The method proposed by the authors is based on sensing the change of dielectric characteristics that occurs in the soil when water escapes from the pipe. The presence of water (whose relative dielectric permittivity is approximately equal to 80) provokes a local, detectable change of the dielectric characteristics of the soil (whose relative dielectric permittivity, in 'dry conditions', does not usually exceed 2–3).

In the present paper, the performance and the practical feasibility of the method are evaluated, thus showing that the proposed leak-detection system yields accurate measurements of the position of the leaks in actual experimental conditions.

A first set of results (case P1) was obtained through experiments on a pilot plant (specifically installed for the purpose of validating the leak-detection system). The plant consisted in a 100 m long buried metal pipe, connected to the water distribution system. In the pipe, two leaks were intentionally created, so that it was possible to assess *i*) the sensitivity of the method as a function of the amount of time in which the leakage had been present; and, most importantly, *ii*) the possibility of pinpointing two simultaneous leaks.

A second set of results was obtained in the context of an extensive experimental leak-detection campaign, performed on a number of already installed metallic pipes (i.e., pipes that were already operating and connected to the water distribution system). TDR measurements

were performed on pipes where a leak-detection crew had preliminarily individuated the possible presence of leaks. For the sake of brevity, only two experimental cases (cases P2, P3) of the aforementioned experimental campaign are reported herein; however, these cases are representative of the typical results obtained on the field.

Finally, with regards to the accurate localization of the leak, the paper also describes a dedicated data-processing algorithm that was specifically implemented to automatically assess the leak positions and to enhance the measurement accuracy. The results reported in this paper were obtained by means of the implemented algorithm.

The paper is organized as follows. Section 2 describes the measurement method, recalling the theoretical background, its practical application, and the employed equations. Section 3 describes the details of the experimental campaign and reports the raw measurement results. Section 4 discusses the method to extract accurate estimates of leaks positions from the TDR waveforms, and the signal processing algorithm employed to obtain the estimates. Section 5 reports and discusses the final quantitative experimental results. Section 6 contains final considerations and conclusions.

2. DESCRIPTION OF THE MEASUREMENT METHOD

2.1. Theoretical Background

As described in [5], the TDR-based leak detection system exploits the physical principles of TDR-based investigation of materials. Generally, this kind of measurements relies on the analysis of the signal that is reflected when an appropriate electromagnetic (EM) signal (typically, a voltage step signal with very fast rise-time) is propagated along a probe (sensing element) inserted in the material under test. The reflected signal, in fact, carries useful information on the dielectric characteristics of the material in which the sensing element is inserted. Therefore, through a suitable data-processing, it is possible to retrieve other intrinsic (qualitative and quantitative) characteristics of the considered material [31].

In TDR measurements, the time-dependent reflection coefficient (ρ) of the material/device under test can be directly displayed as a function of the apparent distance (d^{app}) traveled by the signal that propagates along the sensing element. In turn, ρ is defined as the ratio between the amplitude of the signal that is reflected by the system under test (v_{refl}) and the amplitude of the signal generated by the TDR instrument (v_{inc}) [32]:

$$\rho = \frac{v_{\text{refl}}}{v_{\text{inc}}}, \tag{1}$$

where $-1 \leq \rho \leq +1$, and v_{inc} and v_{refl} are function of d^{app}.

The quantity d^{app} can be considered as the distance that would be traveled by the EM signal in the same interval of time, if the signal were propagating at c, which is the speed of light in vacuum ($c \approx 3 \cdot 10^8\,\text{ms}^{-1}$). d^{app} can be associated to the 'actual' physical length traveled by the signal (d), through the following equation:

$$d^{\text{app}} = \sqrt{\epsilon^{\text{app}}}\, d = \frac{c\, t_{\text{t}}}{2}, \tag{2}$$

where t_{t} is the travel time (round-trip time taken by the signal to travel the physical distance d) and ϵ^{app} is referred to as apparent relative dielectric permittivity of the medium in which the signal propagates [33]. It is worth noting that for low-loss, low-dispersive materials, ϵ^{app} can be considered practically constant in a wide frequency range [34]. The behavior of ρ is strictly associated with the impedance variations along the electrical path traveled by the EM signal. A constant value of ρ means that the dielectric characteristics in that 'portion of path' are practically uniform. Vice versa, variations of ρ indicate that the dielectric characteristics (and, hence, the electrical impedance) change along the traveled electrical path.

2.2. Description of the Measurement System

The upper sketch of Figure 1 shows a schematization of the typical experimental setup. The capital letters indicate the most significant points of the apparatus. The sensing element consists of a two-conductor transmission line (TL): the metal pipe acts as one of the electrodes and a metallic wire (laid down on the road surface, in correspondence of and parallel to the pipe) acts as the second electrode. The reflectometric signal propagates along this two-conductor TL; as a result, the soil becomes the propagation medium.

In presence of a water leak, there will be a local change of the dielectric characteristics of the soil (in fact, water has a high relative dielectric permittivity with respect to soil); therefore, in correspondence of a leak, there will be a change of the reflectogram (generally, a relative minimum is observed). A schematization of a reflectogram in presence of two leaks (at point $E1$ and $E2$) is shown in the lower sketch of Figure 1. For each leak, the reflectogram directly provides, in principle, the apparent position of the leak, $L_{\text{Ei}}^{\text{app}}$; and, through a suitable data-processing, it is possible to retrieve the actual position of the leak, L_{Ei} (in this case, $i = 1, 2$).

From Figure 1, it is also possible to see the other elements of the measurement apparatus. A coaxial cable (with an approximate length of 3 m) is connected to the TDR output port (this allows reducing the

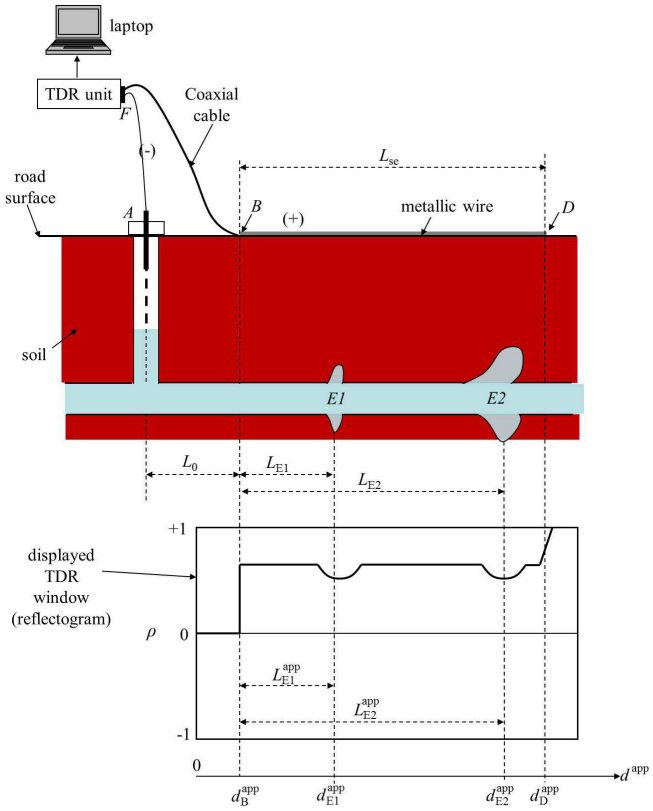

Figure 1. Schematization of the experimental apparatus (upper sketch) and corresponding schematized TDR waveform in presence of two leaks (lower sketch).

effect of undesired impedance mismatches [5]); in turn, the beginning of the metallic wire is connected to the signal pin of the coaxial cable (point B). The length of the metallic wire must be chosen accordingly to the length of pipe that is being inspected; in fact, the length of this wire is the length of the sensing element (L_{se}). The end of the sensing element (i.e., the distal end of the wire, point D) is left open-ended. Finally, a short wire is used to connect the outer conductor of the TDR output port to the valve stem of the underground metal pipe (point A).

With reference to the TDR waveform schematized in Figure 1, the abscissa d^{app} indicates the apparent distance as directly displayed in the reflectogram; the quantity L_{E1}^{app} indicates the apparent distance of the leak $E1$ from point B; and L_{E2}^{app} indicates the apparent distance of

the leak $E2$ from point B.

In normal operating conditions of the pipe (i.e., if no leak is present), ρ would have a constant value along the length of the sensing element. On the other hand, the presence of water associated to a leak causes a local variation of the measured ρ (typically associated to the presence of a relative minimum of the amplitude of the reflected signal).

As reported in [5], the physical position of the i-th leak is individuated through the following equation:

$$L_{\mathrm{Ei}} \approx \frac{L_{\mathrm{Ei}}^{\mathrm{app}}}{\sqrt{\epsilon^{\mathrm{app}}}} = \frac{L_{\mathrm{Ei}}^{\mathrm{app}}}{L_{\mathrm{se}}^{\mathrm{app}}/L_{\mathrm{se}}} = \frac{d_{\mathrm{Ei}}^{\mathrm{app}} - d_{\mathrm{B}}^{\mathrm{app}}}{\left(d_{\mathrm{D}}^{\mathrm{app}} - d_{\mathrm{B}}^{\mathrm{app}}\right)/L_{\mathrm{se}}}. \tag{3}$$

Therefore, to calculate the position of the leak from Eq. (3), it is necessary to determine $d_{\mathrm{B}}^{\mathrm{app}}$, $d_{\mathrm{D}}^{\mathrm{app}}$, and $d_{\mathrm{Ei}}^{\mathrm{app}}$.

On a final note, it is worth mentioning that the employment of the proposed system is not limited to the topology depicted in Figure 1. In particular, the proposed system can also be used for tree networks and branched pipelines; in fact, in these cases, it is enough to appropriately move the metallic wire so as to make it follow the path of the underground pipe that is being tested (even when the pipe has a hairpin bend).

3. DESCRIPTION OF THE EXPERIMENTAL CAMPAIGN AND DISCUSSION OF THE RAW MEASUREMENT RESULTS

3.1. Description of the Apparatus

As schematized in Figure 1, the measurement apparatus includes a TDR instrument, a laptop with the system management software, a metallic wire (which, together with the pipe, forms the sensing element) and the accessories needed for the connections. Since the goal of the work is to demonstrate the practical feasibility of the measurement method, it is important to provide a few practical details for performing correct and successful on-the-field measurements.

Considering the specific application, it is preferable to use a compact, portable TDR instrument, with possibility of being battery-powered. The metallic wire must be anchored to the road surface (with nails or adhesive tape), thus guaranteeing the stability of the mutual distance of the electrodes while the measurement is being performed. As aforementioned, the other electrode (i.e., the underground metal pipe) must be contacted to the reference ground of the output port of the TDR unit. It must be pointed out that this step is particularly

important: in fact, although theoretically obvious, it is non-trivial, and of paramount practical importance, to guarantee the stable electrical continuity between reference ground and metal pipe. Unfortunately, rust on the valve stem may compromise the electrical continuity: therefore, it is always necessary to verify the electrical continuity through a portable multimeter. As a rule of thumb, based on the experience of the authors, to ensure a good electrical continuity, the measured resistance between (A) and (F) must be as low as 1–2 Ω. In case the value of electrical resistance is higher, then it is necessary to abrade with sandpaper the contact point to the pipe.

TDR measurements presented in the paper were performed through the Hyperlabs HL1500. This TDR instrument is a low-cost, portable unit, which makes it particularly useful for on-the-field applications. The HL1500, which is a single-port instrument, generates a step-like signal with a rise time of 200 ps; the amplitude of the signal is 250 mV. The output port has a BNC connector, and the output impedance is 50 Ω. Each TDR measurement reported herein was acquired with 2048 measurements points and was the result of 128 automatic averages.

3.2. Tests on the Pilot Plant

To test the suitability of the proposed system under imposed leakage conditions (in particular, to assess the performance of the system in presence of two leaks) and in correspondence of an increasing amount of leaked water (in particular, in correspondence of an incipient leak), a new metal pipe was installed and connected to the water distribution system. The installed pipe was made of gray cast iron; it was 100 m-long and had a diameter of 150 mm [6]. The topology of the pilot plant was similar to that depicted in the upper sketch of Figure 1, i.e., a straight pipeline with no derivations.

For this experimental case (P1), TDR measurements were performed in three different conditions:

(i) with no leakage;

(ii) causing water leakage from two different points ($E1$ and $E2$);

(iii) causing water leakage from just one point ($E1$).

In order to cause different leak conditions, two holes were intentionally created on the pipe, at reference (known) positions $E1$ and $E2$: in particular, the hole at point $E2$ was significantly bigger than the hole at point $E1$. With reference to the schematization of Figure 1, distances were set as follows: $L_0 \cong 2.0\,\text{m}$; $L_0 + L_{\text{E1}} \cong 29.0\,\text{m}$; and $L_0 + L_{\text{E2}} \cong 60.0\,\text{m}$. After the holes had been created, the pipe was buried approximately 1 m underground.

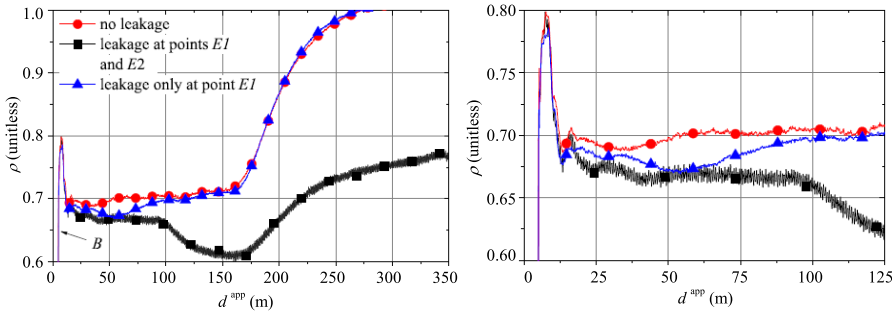

Figure 2. Raw TDR waveforms for the pilot-test case of P1 when no-leak is present (reference waveform), (a) in presence of one leak, and in the simultaneous presence of two leaks, (b) zoom of the beginning of the waveforms.

First operating condition: no leakage. This condition represents the standard operating condition of the 'undamaged' pipe. In fact, although the holes were present, the gate valve was closed (i.e., no water ran through the pipe and, hence, there was no water leakage). The acquired TDR waveform is shown in Figure 2(a) (red curve with circles). From this waveform, it can be seen that the value of ρ is approximately constant at 0.7, until $d^{\text{app}} \approx 160\,\text{m}$, where the end of the sensing element begins to be sensed.

Second operating condition: simultaneous water leakage from two different points. Successively, the gate valve was opened, and water began running through the pipe. As a result, water also began leaking through the holes at $E1$ and $E2$. After approximately three hours, a TDR waveform was acquired (curve with squares in Figure 2(a). It can be seen that two local minima appear, each corresponding to one leakage point. Indeed, the most significant variation of ρ starts to occur at approximately $d^{\text{app}} \approx 100\,\text{m}$, due to the bigger amount of water escaping from the hole at point $E2$. The other minimum begins to be noticeable (at approximately $d^{\text{app}} \approx 47\,\text{m}$), since the water amount in proximity of $E1$ begins to be considerable, thus leading to a corresponding variation of the TDR response.

Third operating condition: water leakage just from one point. For obtaining this condition, the leak at point $E2$ was repaired by placing a split sleeve repair clamp. After the repair, in order not to influence successive measurement, the length of pipe in correspondence of point $E2$ was buried with dry soil (i.e., not with the wet soil that was removed during the intervention repair).

In this condition (i.e., with only one unrepaired hole at point $E1$), the gate valve was opened and water was made run through the pipe for approximately 24 hours. Finally, another TDR waveform was acquired (blue curve with triangles in Figure 2(a)). Two major conclusions can be drawn from this curve: *i*) that the local minimum in correspondence of the leak at point $E1$ is more evident (because of the higher amount of water that had leaked for a total of 27 hours); and most importantly *ii*) that in correspondence of the point $E2$, the value of the reflection coefficient is, practically, equal to that previously measured in the no-leakage condition, as a result of the fact that the leakage was eliminated.

3.3. Tests Performed through an on-the-field Measurement Campaign

Additional experiments were carried out on already-installed metal pipes. In practice, a leak-detection crew had individuated the possible presence of leaks in a number of pipes (the crew had used traditional methods: listening rod, geophones and correlator). Successively, the same pipes were inspected through the proposed TDR-based system. Finally, the presence (or absence) of the 'supposed' leak was verified *ex post* (through excavation during the repair intervention).

The reported experimental cases are referred to as P2 and P3. For each considered case, the same experimental apparatus shown in Figure 1 was used. For P2 and P3, the diameter of the metallic wire was 5 mm and the length (L_{se}) was 98.9 m (chosen according to the length of pipe to be inspected). The length of the coaxial cable was 3 m in all the considered cases. It is worth mentioning that, in both the cases P2 and P3, the considered pipes were straight pipelines, without

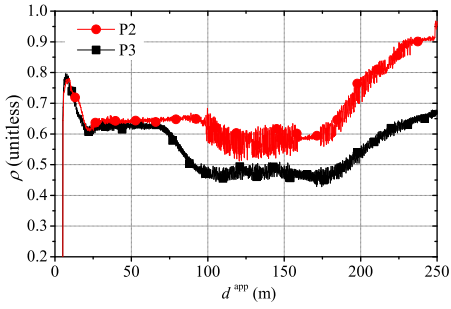

Figure 3. TDR waveforms acquired in the experimental cases P2 and P3.

derivations (at least, in the inspected portions of pipes). Figure 3 shows the results obtained in the experimental cases P2 and P3. It can be seen that there are strong variations caused by large amount of water leakage, which occurs approximately at an apparent distance of 100 m and 80 m, for P2 and P3, respectively. Finally, the open-ended termination (point D) occurs at an apparent distance of approximately 200 m.

4. EVALUATION OF THE POSITION OF THE LEAKS

In the previous section, the points B, D and Ei in the TDR signal have been located quite roughly through a qualitative analysis of the TDR waveform. Nevertheless, to determine the position of the leak using Eq. (3), it is necessary to accurately evaluate the quantities $d_{\mathrm{B}}^{\mathrm{app}}$, $d_{\mathrm{D}}^{\mathrm{app}}$, and $d_{\mathrm{Ei}}^{\mathrm{app}}$. For this purpose, a proper processing of the TDR data must be carried out.

The abscissa $d_{\mathrm{B}}^{\mathrm{app}}$ is easy to determine precisely (i.e., with negligible ambiguity and high repeatability). In fact, it corresponds to the abrupt change in ρ, caused by the high impedance mismatch at the physical point B. In this point, the TDR signal exhibits a clear abrupt jump, with ρ going from a very low value to a positive value (approximately 0.8 in the considered cases).

The abscissae $d_{\mathrm{D}}^{\mathrm{app}}$ corresponds to the end of the transmission line formed by the wire and the pipe; this quantity can be individuated as the maximum of the derivative ρ'. In fact, for an ideal open-circuited termination, the ρ curve in correspondence of the end of the sensing element should be a vertical line that reaches approximately 1. In practical applications, because the soil acts as a load at the end of the sensing element and because of the dissipative effects of the propagation medium (which slows down the electromagnetic signal), the end of the line appears 'smeared'. Generally, the end of the sensing element falls in correspondence of the point where ρ has the maximum positive slope (i.e., at the maximum of ρ').

Finally, the quantity $d_{\mathrm{Ei}}^{\mathrm{app}}$ corresponds to the leakage point. As already seen in the previous section, the leaked water causes the presence of a dip (typically, a local minimum) in the TDR waveform, in correspondence of the leakage point. Based on the shape of this dip, it is possible to make some considerations.

When the dip is not wide, it generally means that the variation of ρ occurs within a limited area; hence, it is reasonable to assume that only a small amount of water has escaped and/or the leak is only incipient. In these cases, $d_{\mathrm{Ei}}^{\mathrm{app}}$ is best inferred as the local minimum of the dip of the ρ curve (or, zero-crossing of the derivative).

On the other hand, when the dip is wide (i.e., it extends for several meters of apparent length), it is reasonable to assume that there is a big amount of escaped water. In this case, the position of the leak is best inferred as the inflection point that leads to the dip in the ρ curve. In fact, the falling portion of the dip in the ρ curve roughly corresponds to the area in which the soil 'starts to be sensed' as wet. This point is individuated as the point with maximum negative slope of ρ (i.e., as the local minimum of ρ') [35, 36]. As will be detailed in the following paragraphs, the experimental results so far have confirmed the aforementioned considerations.

The individuation of the position of points D and Ei directly from the raw TDR waveform (i.e., from the TDR signal as acquired by the instrument) may be quite difficult. In fact, in practical applications, the ρ curve is noisy and the correct interpretation is not a trivial task. As a direct consequence, also calculating the first derivative of the raw TDR signal would lead to a very noisy ρ' curve, which would compromise the accuracy in the evaluation of the involved distances. For these reasons, to obtain a less-noisy ρ curve (and/or a less noisy ρ'), a dedicated algorithm was implemented in MATLAB. The data-processing performed by the algorithm is based on the well-known Nicolson method for the spectral analysis and filtering of step-like signals [37].

The algorithm also includes the operations for calculating the position of the leaks.

4.1. Data Processing for the Automatic Pinpointing of the Leak

In this subsection, the algorithm is described referring to the experimental case P2. The basic operations performed by the algorithm are summarized in Figure 4. It is worth mentioning that, although for the sake of clarity the reported elaboration refers to the presence of only one leak (and the subscript 'i' is dropped), the algorithm can also successfully be used to individuate multiple leaks.

The first step is to select a suitable portion of the TDR waveform, thus windowing out those portions of the signal that do not carry useful information on the position of the leak and that, on the contrary, could jeopardize the FFT-based fitting of the curve.

With regards to the case P2, Figure 5(a) shows the acquired TDR waveform. Since the sensing element begins at point B, the portion of waveform before this point can be discarded. Indeed, because of the presence of impedance mismatch, it is preferable to window out all the portion of the waveform up to the point where the signal appears to have settled to a constant value (point S). The choice of S is not

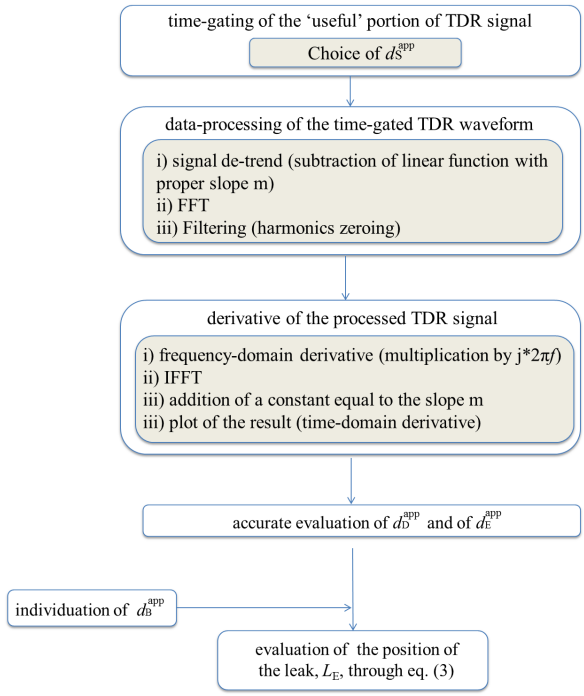

Figure 4. Schematized diagram of the steps of algorithm for estimating the position of the leak.

critical, provided that it excludes only the region of initial oscillations due to the impedance mismatch (and not to actual variations in the soil permittivity).

Moreover, for this specific case, it can be seen that at approximately $d^{app} = 250\,m$ there is a singularity in the acquired TDR waveform. Also this portion of waveform does not carry useful information and can be discarded (in fact, the reflection of the end of the sensing element occurs well before this point). In summary, only the portion between the dashed red lines of Figure 5(a) is considered in the subsequent processing.

The gated TDR signal is then transformed into the frequency domain and, to reduce the effect of noise, the harmonics attributable to noise are discarded. However, for performing this operation without losing information in the time-domain/frequency domain transformation, the principle of the Nicolson method is followed. Basically, the Nicolson method consists in the fast Fourier transform (FFT) analysis of the signal after subtracting a linear ramp, so that

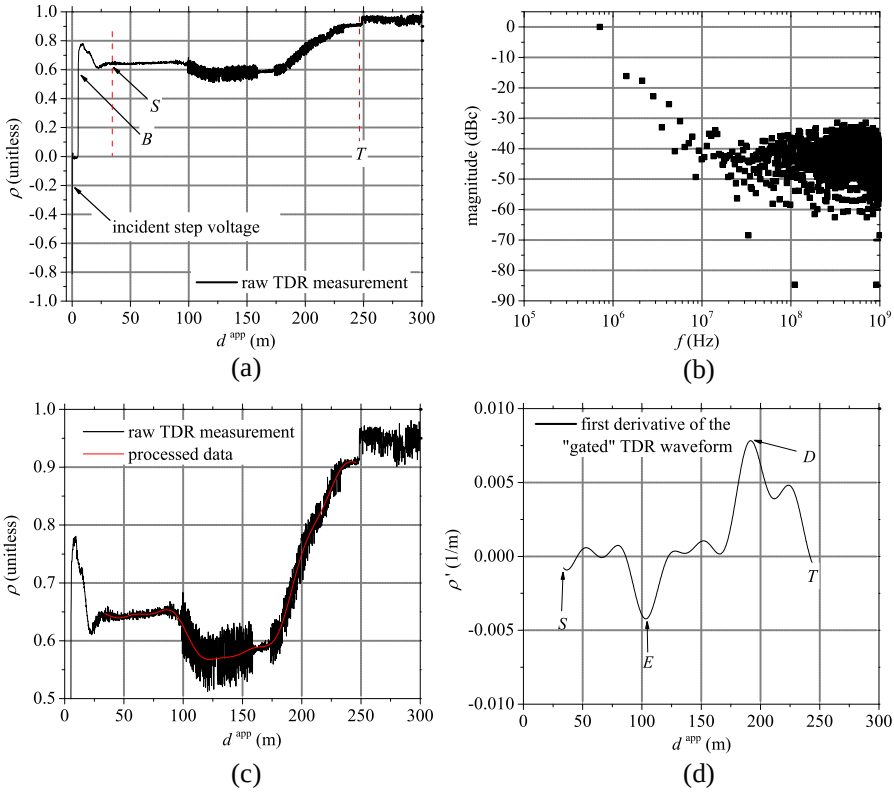

Figure 5. Steps of the data-processing performed through the MATLAB algorithm for the experimental case P2: (a) raw TDR waveform. The dashed red line indicates the 'useful' portion of the signal; (b) frequency spectrum associated to gated TDR signal; (c) comparison between the raw TDR waveform and the IFFT of the first N_h harmonics of the frequency spectrum; (d) first derivative of the processed TDR waveform.

the first and the last samples of the analyzed waveform have the same value (the inherent discontinuity of the step-like signal is therefore eliminated).

After applying the signal de-trend of the Nicolson method, the FFT is evaluated, thus obtaining the spectral content of the de-trend of the signal, shown in Figure 5(b). The obtained frequency spectrum shows the presence of considerable noise at high frequency; therefore, the useful portion of the frequency spectrum is represented only by those harmonics that are not overwhelmed by noise. Indeed, there is

not a fixed rule on the number of harmonics (N_{h}) to be considered 'useful'; as a rule of thumb it is important to consider only those harmonics that are clearly distinguishable from noise.

Once the N_{h} harmonics are chosen, the inverse fast Fourier transform (IFFT) is applied, then the Nicolson scaling is removed and finally the corresponding filtered TDR waveform is obtained. Figure 5(c) compares the raw TDR waveform with the filtered TDR waveform. It can be seen that in the filtered waveform, noise is dramatically reduced.

Successively, the derivative of the signal is evaluated, and $d_{\mathrm{D}}^{\mathrm{app}}$ is assessed as the local maximum of ρ' (Figure 5(d)). As for the quantity $d_{\mathrm{E}}^{\mathrm{app}}$, based on the shape of the dip in correspondence of the leak in the P2 case, it was calculated as the local minimum of ρ'.

All these quantities are finally used by the algorithm to calculate the physical position of the leak, L_{E}, through Eq. (3).

It should be pointed out that the derivative in the time domain might be also calculated by taking the IFFT of the signal and then the differences between consecutive samples. Nevertheless, this might introduce errors; in fact, the sampling interval must be assumed to be small enough to substitute an infinitesimal increment. These errors (which are often negligible in many practical case) is totally absent when calculating the derivative in the frequency domain (multiplication of the harmonics at frequency f_{h} by $j2\pi f_h$ (where $j = (-1)^{1/2}$), and then taking the IFFT).

5. FINAL EXPERIMENTAL RESULTS

The processing algorithm described in the previous section was applied for determining the position of the leaks in all the reported experimental cases. For each case, Table 1 summarizes the length of

Table 1. Summarized results in the pinpointing of the leak for the reported experimental cases P1, P2, and P3.

Experimental case	L_{se} (m)	N_{h}	$L_{\mathrm{E1}}^{\mathrm{act}}$ (m)	$L_{\mathrm{E1}}^{\mathrm{eval}}$ (m)	$L_{\mathrm{E2}}^{\mathrm{act}}$ (m)	$L_{\mathrm{E2}}^{\mathrm{eval}}$ (m)
P1 (2 leaks)	96.9	14	27	20.1*	58	54.3
P1 (1 leak)	96.9	10	27	27.9*	-	-
P2	98.9	6	53.6	51.4	-	-
P3	98.9	7	42	39.9	-	-

**value calculated as the local minimum of the ρ curve

the used wire (L_{se}); the actual position of the i-th leak as imposed or as verified after excavation (L_{Ei}^{act}); the number of harmonics included in the data processing (N_h); and the position of the i-th leak as evaluated through the described algorithm (L_{Ei}^{eval}).

Results show that there is an overall good agreement between the evaluated position and the actual position of the leaks. This demonstrates that, in practical applications, the proposed TDR-based system can be successfully used to determine the unknown position of leaks in already-installed underground metal pipes.

It should be pointed out that, except for the leak $E1$ in P1 (in two different cases indicated with an asterisk), the positions of the leaks reported in Table 1 were obtained by searching for the local minimum of the ρ' curve. In fact, as mentioned in[5], in presence of profuse leakage (big amount of water escaped and/or the leak has been present for longer times), the position of the leak is individuated accurately as the local minimum of the ρ' (i.e., the inflection point that leads to the local minimum of ρ). This is the condition of cases P2, P3, in which the leaks had been present for a long time before the TDR measurements were performed. This also occurs for leak $E2$ of case P1: in fact, the hole provoked in $E2$ was bigger and, similarly to the previous cases, it led to a much bigger amount of escaped water. Basically, the reason is that the big amount of water slows down the propagation of the signal.

On the other hand, in presence of an incipient leak (in which there is little water and/or water has had little time to diffuse through the soil), the position of the leak is best inferred as the local minimum of the ρ curve. This is the case of leak $E1$ in the P1 case, in which a small hole was provoked and TDR measurements were performed only hours later.

As a further demonstration of these considerations, it is worth mentioning that when the position of the leak at $E1$ in the P1 case was evaluated by searching for the local minimum of ρ (rather than searching for the local minimum of ρ'), the value of L_E^{eval} was 10 m in the case of one leak and 14 m in the presence of two leaks: both these values are quite different from the actual position of the leak (27 m).
It is important to mention a specific aspect regarding the evaluation of ϵ^{app} for solving Eq. (3). The fact that the obtained results are affected only by a small error (when comparing the evaluated position of the leak with the reference position) demonstrates that, in each case, having considered the soil as homogeneous (and, hence, considering the overall ϵ^{app} practically constant, rather than using a specific dielectric mixing model for describing the dielectric characteristics of the soil), does not represent a problematic source of error.

Finally, with respect to the practical implementation of the

method, it is worth making some considerations on the performance of the proposed system in presence of or after rain. Although the proposed leak-detection method is based on detecting changes in the value of the soil permittivity, in general, the performance of the proposed system is expected not to be dramatically influenced by rain (unless the street is flooded with water). Clearly, the performance of the system after heavy rain depends on how much the soil gets soaked with water. As a rule of thumb, it can be said that the system works correctly as long as the permittivity of the soil in proximity of the leak is sufficiently different from the permittivity of the surrounding soil. Unfortunately, a definitive value may not be given, because it is not trivial to measure a-priori the permittivity of the soil in proximity of the leak. However, in the experience of the authors, the typical scenarios that may occur can be grouped into two main categories:

1) If the road surface on which the metallic wire is laid down is asphalt, then water is often drained by the asphalt itself and does not penetrate (excessively) the soil below. In such a condition, the performance of the system is not influenced by rain (similarly, if the road surface is made with stone, water does not penetrate below).

2) If the road surface is soil (for example, in countryside areas) then the penetration of water due to rain might be considerable (depending on the soil structure) and the performance of the system, in such circumstance, may not be adequate. However, in this case, in order to understand whether the condition of the soil allows an optimal performance of the leak-detection method, it is possible to obtain a prompt estimation of the approximate value of permittivity of the soil; hence, deducing the amount of rain water that has soaked the soil (if any). Such a measurement can be done preliminarily with the same TDR instrument that would be used for inspecting the pipe. In fact, it is possible to use the well-known three-rod probes connected to the TDR instrument and inserted in the soil [38]. This preliminary measurement could be performed every time that there are doubts on whether the (dielectric/moisture) characteristics of the soil may compromise the accuracy of the method.

6. CONCLUSION

In this work, the experimental validation of an innovative method for pinpointing water leaks in underground metal pipes was presented. The reported experimental data were obtained from measurements on a pilot plant (in which leaks were intentionally created at known positions and for a known time) and through on-the-field measurements (in these cases, the actual position of the leaks was found after

excavation). Additionally, the processing algorithm for the automatic evaluation of the position of the leak was described in detail. The experimental cases reported herein showed that the proposed system can be used to accurately pinpoint the position of the leak, also in presence of multiple leaks along the same length of pipe under investigation. It must be highlighted that the proposed system dramatically reduces the inspection time required by traditional methods and, additionally, it can be employed regardless of the operating conditions of the pipe (i.e., no need for high water pressure). The reported results, in particular, demonstrate that, by employing the proposed TDR method, it is possible to inspect hundreds-of-meters long buried pipes in a single shot.

REFERENCES

1. Farley, M. and S. Trow, *Losses in Water Distribution Networks*, 1st Edition, IWA Publishing, London, UK, 2003.
2. Puust, R., Z. Kapelan, D. A. Savic, and T. Koppel, "A review of methods for leakage management in pipe networks," *Urban Water Journal*, Vol. 7, No. 1, 25–45, 2010.
3. Wang, G., D. Dong, and C. Fang, "Leak detection for transport pipelines based on autoregressive modeling," *IEEE Transactions on Instrumentation and Measurement*, Vol. 42, No. 1, 68–71, 1993.
4. Bimpas, M., A. Amditis, and N. Uzunoglu, "Detection of water leaks in supply pipes using continuous wave sensor operating at 2.45 GHz," *Journal of Applied Geophysics*, Vol. 70, No. 3, 226–236, 2010.
5. Cataldo, A., G. Cannazza, E. De Benedetto, and N. Giaquinto, "A new method for detecting leaks in underground water pipelines," *IEEE Sensors Journal*, Vol. 12, No. 6, 1660–1667, 2012.
6. Cataldo, A., G. Cannazza, E. De Benedetto, and N. Giaquinto, "Performance evaluation of a TDR-based system for detection of leaks in buried pipes," *Proceedings of IEEE 2012 International Instrumentation and Measurement Technology Conference*, 792–795, Graz, Austria, May 2012.
7. "Apparatus and method for detection and localization of leaks and faults in underground pipes," WO Patent Pending BA2011A000034, 2011.
8. Cataldo, A., L. Catarinucci, L. Tarricone, F. Attivissimo, and A. Trotta, "A frequency-domain method for extending TDR performance in quality determination of fluids," *Measurement Science and Technology*, Vol. 18, No. 3, 675–688, 2007.

9. Hager, III, N. E., "Broadband time-domain-reflectometry dielectric spectroscopy using variable-time-scale sampling," *Review of Scientific Instruments*, Vol. 64, No. 4, 887–891, 1994.
10. Moradi, G. and A. Abdipour, "Measuring the permittivity of dielectric materials using STDR approach," *Progress In Electromagnetics Research*, Vol. 77, 357–365, 2007.
11. Nozaki, R. and T. K. Bose, "Broadband complex permittivity measurements by time-domain spectroscopy," *IEEE Trans. Instrum. Meas.*, Vol. 39, No. 6, 945–951, 1990.
12. Cataldo, A., L. Catarinucci, L. Tarricone, F. Attivissimo, and E. Piuzzi, "A combined TD-FD method for enhanced reflectometry measurements in liquid quality monitoring," *IEEE Transactions on Instrumentation and Measurement*, Vol. 58, No. 10, 3534–3543, 2009.
13. Piuzzi, E., A. Cataldo, and L. Catarinucci, "Enhanced reflectometry measurements of permittivities and levels in layered petrochemical liquids using an 'in-situ' coaxial probe," *Measurement*, Vol. 42, No. 5, 685–696, 2009.
14. Cataldo, A., E. Piuzzi, G. Cannazza, E. De Benedetto, and L. Tarricone, "Quality and anti-adulteration control of vegetable oils through microwave dielectric spectroscopy," *Measurement*, Vol. 43, No. 8, 1031–1039, 2010.
15. Cataldo, A., E. Piuzzi, G. Cannazza, and E. De Benedetto, "Dielectric spectroscopy of liquids through a combined approach: evaluation of the metrological performance and feasibility study on vegetable oils," *IEEE Sensors Journal*, Vol. 9, No. 10, 1226–1233, 2009.
16. Cataldo, A., E. Piuzzi, G. Cannazza, and E. De Benedetto, "Classification and adulteration control of vegetable oils based on microwave reflectometry analysis," *Journal of Food Engineering*, Vol. 112, No. 4, 338–345, 2012.
17. Liu, Y., L. Tong, W.-X. Zhu, Y. Tian, and B. Gao, "Impedance measurements of nonuniform transmission lines in time domain using an improved recursive multiple reflection computation method," *Progress In Electromagnetics Research*, Vol. 117, 149–164, 2011.
18. Bishop, J., D. Pommerenke, and G. Chen, "A rapid-acquisition electrical time-domain reflectometer for dynamic structure analysis," *IEEE Transactions on Instrumentation and Measurement*, Vol. 60, No. 2, 655–661, 2011.
19. Furse, C., P. Smith, and M. Diamond, "Feasibility of reflectometry for nondestructive evaluation of prestressed concrete anchors,"

IEEE Sensors Journal, Vol. 9, No. 11, 1322–1329, 2009.

20. Griffiths, L. A., R. Parakh, C. Furse, and B. Baker, "The invisible fray: A critical analysis of the use of reflectometry for fray location," *IEEE Sensors Journal*, Vol. 6, No. 3, 697–706, 2006.
21. Schuet, S., D. Timucin, and K. Wheeler, "A model-based probabilistic inversion framework for characterizing wire fault detection using TDR," *IEEE Transactions on Instrumentation and Measurement*, Vol. 60, No. 5, 1654–1663, 2011.
22. Scheuermann, A. and C. Huebner, "On the feasibility of pressure prole measurements with time-domain reflectometry," *IEEE Transactions on Instrumentation and Measurement*, Vol. 58, No. 2, 467–474, 2009.
23. O'Connor, K. M. and C. H. Dowding, *GeoMeasurements by Pulsing TDR Cables and Probes*, CRC Press, UK, Jan. 1999.
24. Cataldo, A., G. Monti, E. De Benedetto, G. Cannazza, and L. Tarricone, "A noninvasive resonance-based method for moisture content evaluation through microstrip antennas," *IEEE Transactions on Instrumentation and Measurement*, Vol. 58, No. 5, 1420–1426, 2009.
25. Cataldo, A., G. Monti, G. Cannazza, E. De Benedetto, and L. Tarricone, "A non-invasive approach for moisture measurements through patch antennas," *Proc. IEEE Int. Instrum. Meas. Technol. Conf.*, 1012–1015, Victoria, BC, May 2008.
26. Serdyuk, V. M., "Dielectric study of bound water in grain at radio and microwave frequencies," *Progress In Electromagnetics Research*, Vol. 84, 379–406, 2008.
27. Cataldo, A., G. Monti, E. De Benedetto, G. Cannazza, L. Tarricone, and L. Catarinucci, "Assessment of a TD-based method for characterization of antennas," *IEEE Transactions on Instrumentation and Measurement*, Vol. 58, No. 5, 1412–1419, 2009.
28. Cataldo, A., G. Monti, E. De Benedetto, G. Cannazza, L. Tarricone, and L. Catarinucci, "A comparative analysis of reflectometry methods for characterization of antennas," *Proc. IEEE Int. Instrum. Meas. Technol. Conf.*, 240–243, Victoria, BC, May 2008.
29. Cataldo, A., G. Monti, E. De Benedetto, and G. Cannazza, "A reliable low-cost method for accurate characterization of antennas in time domain," *Metrology and Measurement Systems*, Vol. 15, No. 4, 571–583, 2008.
30. Okhovvat, M. and R. Fallahi, "Measurement of antenna reflection

coefficient in time domain," *Proc. 11th International Conference on Mathematical Methods In Electromagnetic Theory*, 328–330, Kharkiv, Ukraine, Jun. 2006.

31. Cataldo, A. and E. De Benedetto, "Broadband reflectometry for diagnostics and monitoring applications," *IEEE Sensors Journal*, Vol. 11, No. 2, 451–459, 2011.
32. Dyer, S. A., *Survey of Instrumentation and Measurement,* John Wiley & Sons Inc., USA, 2001.
33. Mohamed, A. M. O., *Principles and Applications of Time Domain Electrometry in Geoenvironmental Engineering*, Taylor & Francis Group, Great Britain, 2006.
34. Robinson, D. A., S. B. Jones, J. M. Wraith, D. Or, and S. P. Friedman, "A review of advances in dielectric and electrical conductivity measurement in soils using time domain reflectometry," *Vadose Zone Journal*, Vol. 2, No. 4, 444–475, 2003.
35. Chung, C. C. and C. P. Lin, "Apparent dielectric constant and effective frequency of TDR measurements: Influencing factors and comparison," *Vadose Zone Journal*, Vol. 8, No. 3, 548–556, 2009.
36. Robinson, D. A., M. G. Schaap, D. Or, and S. B. Jones, "On the effective measurement frequency of time domain reflectometry in dispersive and nonconductive dielectric materials," *Water Resources Research*, Vol. 41, No. 2, W02 007.1–W02 007.9, 2005.
37. Nicolson, A. M., "Forming the fast fourier transform of a step response in time-domain metrology," *Electronic Letters*, Vol. 9, No. 14, 317–318, 1973.
38. Cataldo, A., G. Cannazza, E. De Benedetto, L. Tarricone, and M. Cipressa, "Metrological assessment of TDR performance for moisture evaluation in granular materials," *Measurement*, Vol. 42, No. 2, 254–263, 2009.